In situ high-temperature characterization of AlN-based surface acoustic wave devices

T. Aubert, Jochen Bardong, Ouarda Legrani, O. Elmazria, M. Badreddine Assouar, Gudrun Bruckner, Abdelkrim Talbi

Journal of Applied Physics

In situ high-temperature characterization of AlN-based surface acoustic wave devices

Cite as: J. Appl. Phys. **114**, 014505 (2013); https://doi.org/10.1063/1.4812565
Submitted: 27 March 2013 • Accepted: 13 June 2013 • Published Online: 03 July 2013

Thierry Aubert, Jochen Bardong, Ouarda Legrani, et al.

In situ high-temperature characterization of AlN-based surface acoustic wave devices

Thierry Aubert,[1] Jochen Bardong,[2] Ouarda Legrani,[3] Omar Elmazria,[3]
M. Badreddine Assouar,[3,4] Gudrun Bruckner,[2] and Abdelkrim Talbi[5]
[1]*Université de Savoie, Laboratoire Symme, Annecy-le-Vieux, France*
[2]*Carinthian Tech Research (CTR), Villach/St. Magdalen, Austria*
[3]*Institut Jean Lamour (IJL), UMR 7198 CNRS-Nancy Université, Vandoeuvre-lès-Nancy, France*
[4]*International Joint Laboratory (UMI 2958) CNRS-GIT, Georgia Institute of Technology, Atlanta, Georgia 30332–0605, USA*
[5]*Institut d'Electronique, de Microélectronique et de Nanotechnologie (IEMN), Lille, France*

(Received 27 March 2013; accepted 13 June 2013; published online 3 July 2013)

We report on *in situ* electrical measurements of surface acoustic wave delay lines based on AlN/sapphire structure and iridium interdigital transducers between 20 °C and 1050 °C under vacuum conditions. The devices show a great potential for temperature sensing applications. Burnout is only observed after 60 h at 1050 °C and is mainly attributed to the agglomeration phenomena undergone by the Ir transducers. However, despite the vacuum conditions, a significant oxidation of the AlN film is observed, pointing out the limitation of the considered structure at least at such extreme temperatures. Original structures overcoming this limitation are then proposed and discussed. © *2013 AIP Publishing LLC*. [http://dx.doi.org/10.1063/1.4812565]

I. INTRODUCTION

Surface acoustic waves (SAW) technology constitutes a promising way to achieve passive wireless sensors able to operate at high temperatures ranging from 200 °C to estimated 1000 °C.[1] The choice of the constitutive materials is then critical. Few piezoelectric media can be considered for applications above 500 °C. Currently, langasite (LGS) is considered as the best-suited substrate for harsh environments. Pereira da Cunha *et al*. have demonstrated that LGS-based SAW devices can be operated for at least $5^1/_2$ months. at 800 °C,[2] and in our previous work we have recorded a SAW signal up to 1140 °C on such devices.[3] However, LGS suffers from some drawbacks such as rapidly increasing propagation losses with frequency and temperature. This confines the operating frequency of high-temperature wireless LGS-devices to the couple hundred MHz range.[4,5] LGS also undergoes, as many oxides, strong O losses accompanied by Ga ones under high-temperature low-oxygen conditions.[3] Thus, it would be valuable to find some alternative piezoelectric materials able to advantageously replace LGS for some specific purposes. In this perspective, aluminium nitride (AlN) thin films were identified as such many years ago.[6,7] Indeed, AlN retains its piezoelectricity up to at least 1150 °C[8] and is chemically stable up to 1040 °C under ultra-high vacuum conditions.[9] Its main drawback concerns its sensitivity to oxidation in air atmosphere from 700 °C.[10] Moreover, showing the highest SAW velocity among the piezoelectric materials, AlN is particularly suited to perform high-frequency devices, when combined with fast substrates such as sapphire or diamond.[11,12] Several recent studies have experimentally confirmed the potential of AlN for high-temperature SAW applications. Lin *et al*. successfully operated AlN Lamb wave resonators up to 700 °C.[13] Bruckner *et al*. studied between room temperature and 625 °C SAW delay lines based on AlN/sapphire bilayer structure, with an AlN relative thickness of about 10%. The devices are described as well suited for temperature sensor applications with a large first-order temperature coefficient of delay (TCD) of +67 ppm/°C and a rather weak second-order one (+18 ppb/°C^2). Besides, stable frequency and time responses were observed all along a 45-h-long period at 625 °C.[14] We also provided the same conclusions about very similar devices examined up to 500 °C.[10] Again, a large and quasi-constant sensitivity to the temperature was observed, with a first-order temperature coefficient of frequency (TCF) equal to −68 ppm/°C at 20 °C and −80 ppm/°C at 500 °C. On the other hand, this study evidenced a constant increase of insertion losses (IL) of 1 dB per 100 °C. This phenomenon was attributed to the prevalence of the propagation losses increase with temperature over the observed amelioration of the electromechanical coupling K^2 of the structure.[10]

The aim of the present study is to determine the potential of AlN/sapphire bilayer structure for SAW applications beyond 700 °C. To do so, SAW delay lines are characterized by *in situ* RF electrical measurements between the ambient and temperatures above 1000 °C. The impact of the exposure to such high temperatures on the morphology and the chemical composition of the devices is then analyzed and discussed. Based on these results, original structures that could overcome the observed limitations are suggested.

II. EXPERIMENTAL

1.3 μm-thick (002) AlN thin films were grown on c-cut sapphire substrates by sputtering method. An optimization of the deposition parameters was conducted to obtain high-quality AlN films regarding SAW applications, i.e., films with low stress, high (002) orientation, and surface roughness in the order of few nanometers. The microstructure of

the as-deposited films was investigated by X-ray diffraction (XRD) and transmission electron microscopy (TEM), while atomic force microscopy (AFM) gave access to the morphology.

To perform interdigital transducers (IDTs) circumventing the limitations of platinum, 10 nm-thick titanium as an adhesion layer and 100 nm-thick iridium films as electrodes were deposited by e-beam evaporation.[3,15] SAW delay lines were then fabricated by photolithography and ion beam etching. The devices were constituted of two identical IDTs with 50 pairs of fingers and a wavelength λ fixed to 14 μm, resulting in a relative AlN layer thickness of 9%. The IDT center spacing, acoustic aperture, and finger width to space ratio are 65λ, 27λ, and 1:1, respectively. The SAW propagation path was along the X direction of the sapphire substrate. These SAW devices were first characterized at room temperature on a wafer prober. Then, they were investigated at higher temperatures using a specific setup. To do so, the SAW devices are first bonded with 25 μm Pt wires to platinum foil strips that are attached on a chip carrier made from a machinable Rescor^{TM} ceramic platelet (Fig. 1(a)). This chip carrier is clamped to an RF signal cables pair able to withstand high temperatures, whose end is fixed to a niobium block. Clamping is ensured via a main flat spring, several small molybdenum springs, and a lid that allows electrical contact between the RF cables and the chip carrier platinum strips with mechanical pressure only (Figs. 1(b)–1(d)). The setup finally consists of four different sets of such semirigid coaxial RF cables pairs ended with a nobium hull containing the chip carrier (Figs. 1(e) and 1(f)), which are inserted inside a tubular furnace (Fig. 1(g)). Thus, this setup allows the RF high-temperature characterization of 4–8 SAW test structures at once (4 if S_{21} parameters are required and 8 if S_{11} ones are enough). A more complete description of this setup can be found in Ref. 16. In a first stage, the devices were gradually heated from room temperature to 1050 °C in 15 h. The second step of the experiment consisted in a plateau at this last temperature until reaching the device burnout. Vacuum conditions (pressure: 2.10^{-4} mbar) were chosen as both AlN and Ir oxidize above 700 °C in air atmosphere.[10,17] The morphology and chemical composition of the investigated devices surface were analyzed by scanning electron microscopy (SEM) coupled to energy-dispersive X-ray spectroscopy (EDXS). Slices of the devices were obtained by focused ion beam etching (FIB) to perform cross-sectional TEM micrographs.

III. RESULTS AND DISCUSSIONS

A. As-deposited AlN films

XRD measurements revealed that the optimized (002) AlN films are stress-free while being highly textured out of plane, with a full width at half-maximum (FWHM) of the (002) rocking curve as low as 0.26° (Fig. 2(a)). The films are also textured in the plane as shown by TEM diffraction pattern (Fig. 2(b)). The grain size, obtained by AFM, is close to 30 nm (Fig. 2(c)). The surface roughness of the films with an rms value of 8 Å is suitable for SAW applications. The optimization process of the deposition parameters is fully described in Ref. 18. The operating frequency of the SAW devices based on these films and iridium IDTs, as described

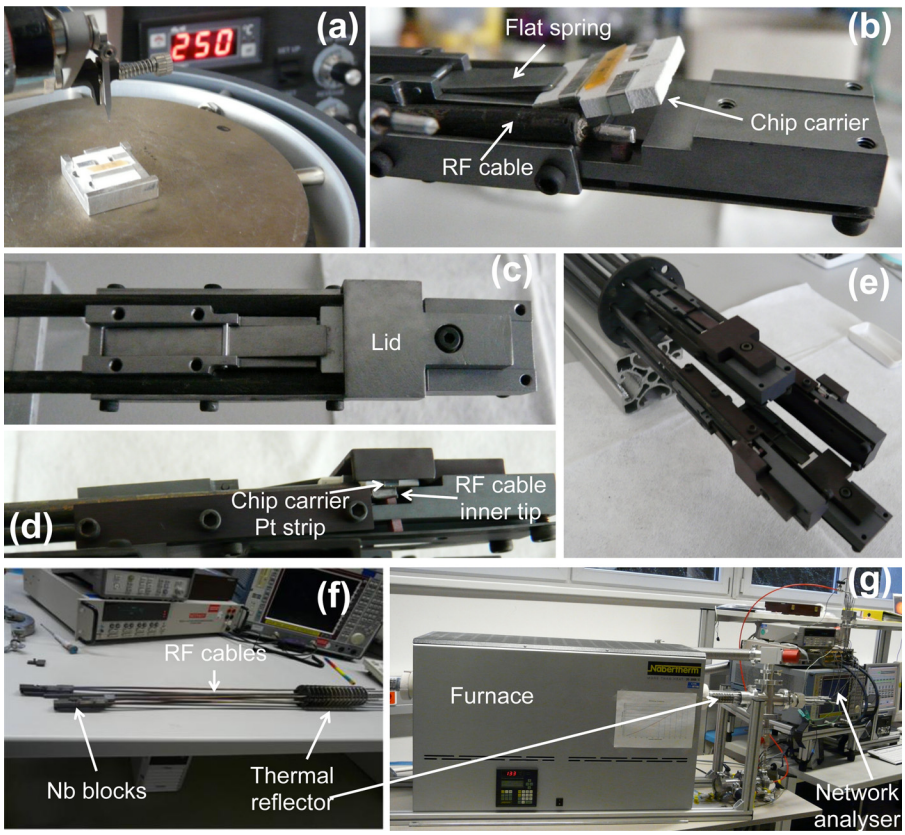

FIG. 1. Description of the high-temperature RF characterization setup. (a) An orange colored langasite device about to be bounded to the chip carrier. (b) A chip carrier just placed inside the Nb block. The flat spring on the left bends it slightly upwards. The orange colored langasite device can be seen on top of the carrier, as the platinum foil strips around the carrier and the platinum plated inner tip of the RF cable. (c), (d) Respectively, top and cross-section views of one set of RF cables pair ended with a Nb hull containing the chip carrier The lid is now closed, pushing the chip carrier down to ensure electrical contact with the RF cables. (e), (f) Views of the setup showing the four sets of RF cables pair ended with a Nb hull. (g) An overview of the complete high-temperature RF characterization setup.

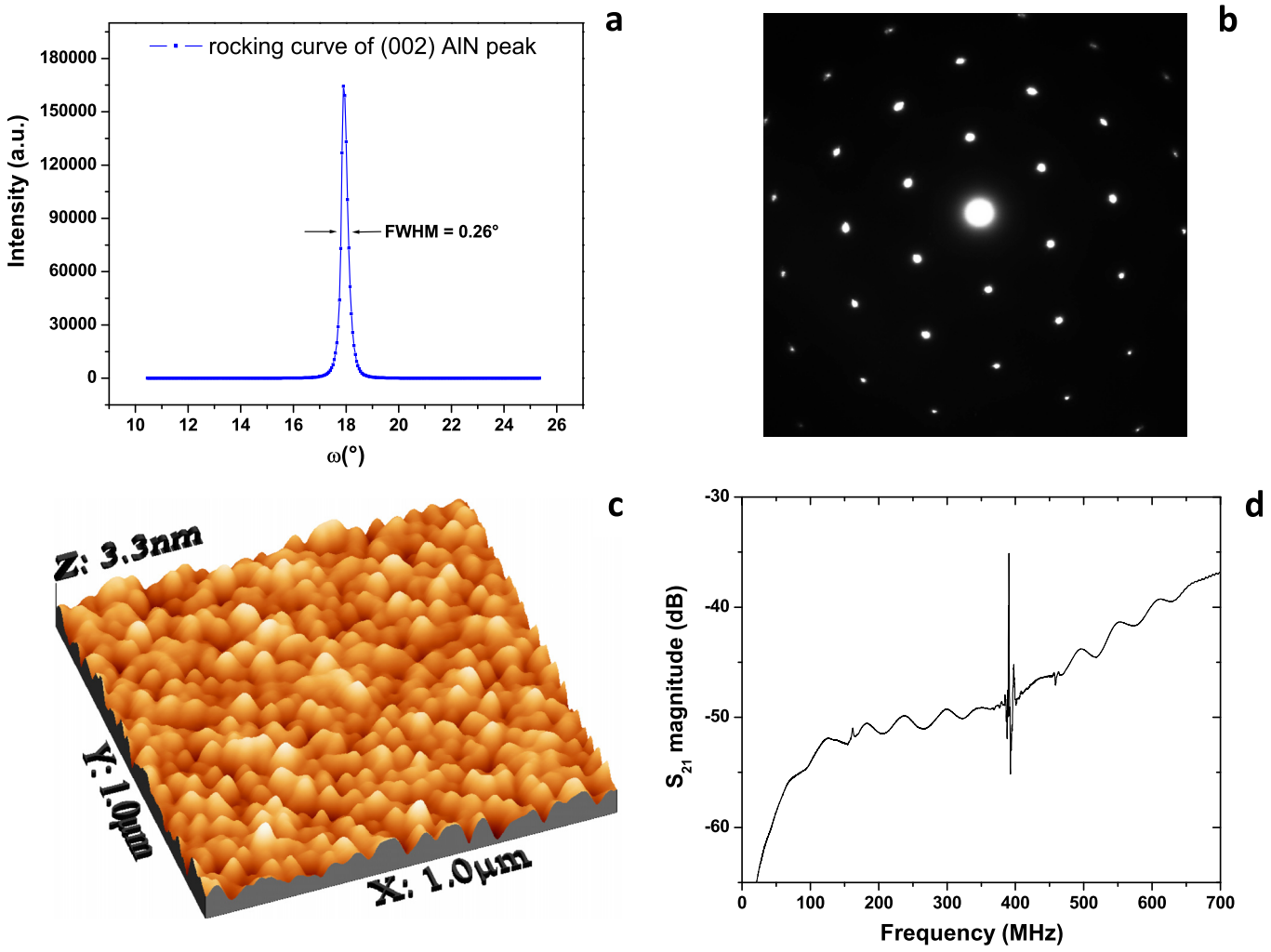

FIG. 2. (a) Rocking curve for the (002) plans in the optimized AlN films. (b) Selected area electronic diffraction (SAED) pattern of the optimized AlN films. (c) 3D AFM image of the optimized AlN films. (d) Frequency response (S_{21} magnitude) of a SAW delay line based on optimized AlN/sapphire structure and Ir IDTs with 14 μm periodicity.

in Sec. II, is closed to 392 MHz, with insertion losses equal to −35 dB and a rejection value of 13 dB (Fig. 2(d)).

B. High-temperature RF characterization of AlN/sapphire devices

This study fully confirms the results reported in literature about the behavior of AlN/sapphire-based SAW devices up to 700 °C (Refs. 10 and 14) and extends them to temperatures as high as 1000 °C. Indeed, as shown in Fig. 3, the investigated delay lines exhibit a large and quasi-linear sensitivity to the temperature in the whole considered temperature range, with TCF values equal to −71 ppm/°C and −12 ppb/°C^2 for the first and second order, respectively, the reference temperature being 20 °C. Moreover, the potential of AlN/sapphire bilayer structure for SAW temperature sensing applications is strengthened by the fact that in the same time, IL are fairly constant with variations below 3 dB (Figs. 3 and 4). The initial increase of IL between room temperature and 500 °C is consistent with the results presented in Ref. 10. It is followed by an unforeseen diminution: IL practically recover the initial value between 750 °C and 850 °C. One can assume that this phenomenon is related to

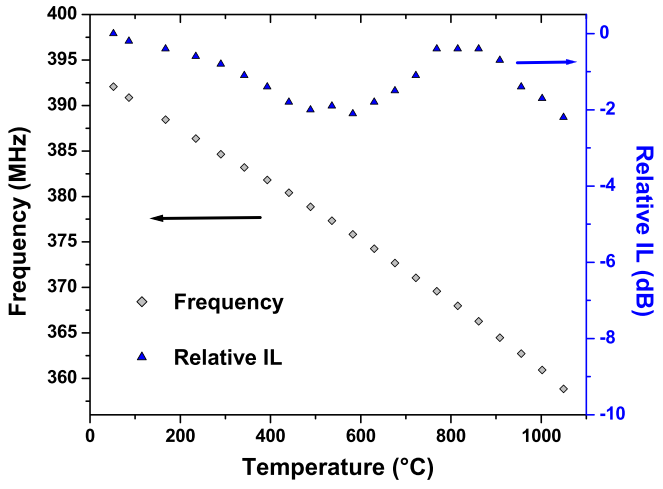

FIG. 3. Frequency-temperature law (grey diamonds) and IL evolution (blue triangles) of Ir/AlN/sapphire SAW delay lines during the 15 h-long heating between 20 °C and 1050 °C. IL values are given relatively to their level at room temperature. Operating frequencies and IL values were obtained from time-gated S_{21} measurements.

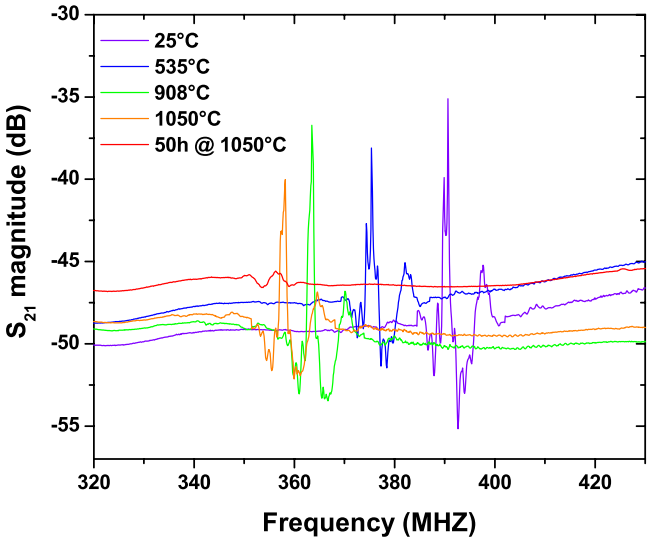

FIG. 4. Raw frequency responses (S_{21} magnitude) of an Ir/AlN/sapphire SAW delay line obtained at different temperatures: 25 °C, 535 °C, 908 °C, 1050 °C and after 50 h at this last temperature.

the fact that the continuous increase of K^2 with temperature described in Ref. 10 certainly goes on above 500 °C and maybe even accelerates. This improvement of K^2 with temperature can be explained, on one hand, by steady softening of AlN/sapphire bilayer structure—as evidenced by the quasi-constant negative TCF value. On the other hand, the significant difference between the expansion coefficients of AlN and sapphire causes an increasing stress in the AlN film when the temperature rises. Consequently, the piezoelectric coefficients of AlN thin films should increase with temperature, which was experimentally demonstrated up to 300 °C.[19] At higher temperatures, in particular during the final plateau at 1050 °C, a permanent increase of IL can be observed, leading to the signal loss after 60 h at this extreme temperature. This phenomenon indicates a progressive deterioration of the device, which is confirmed by the frequency drift occurring during this temperature plateau (Fig. 5).

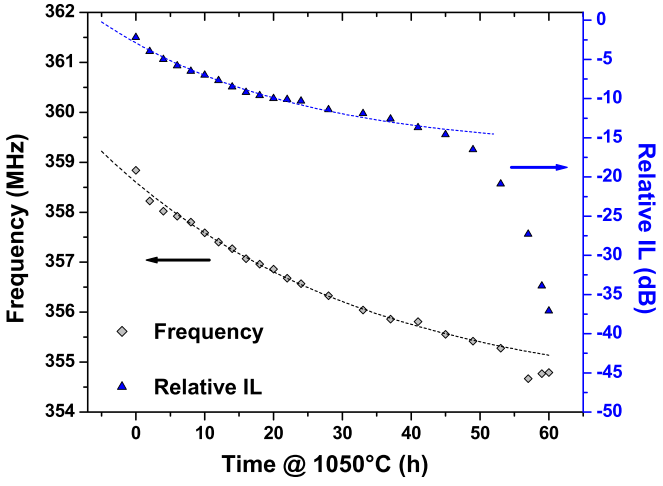

FIG. 5. Evolution with time of operating frequency (grey diamonds) as well as IL (blue triangles) during the final plateau at 1050 °C. Black and blue dashed curves are exponential decay fitting curves of the operating frequency and IL evolution, respectively. Operating frequencies and IL values were obtained from time-gated S_{21} measurements.

C. Material analyses

One clear reason of the final device failure can be directly seen on post-experiment SEM images. The Ir IDTs underwent agglomeration phenomena during the high-temperature exposure, which broke the electrical continuity of the transducers (Fig. 6(a)). This was expected as the temperature of the 60-h-long plateau, i.e., 1050 °C, is very close to the Tamman temperature of Ir, equal to 1080 °C. Tamman temperature gives a rough estimation of the onset temperature of volume diffusion phenomena in metals, which lead in a couple of hours to such agglomeration phenomena in thin films.[20] One can also note on SEM images the apparition of nanostructures on the surface of the substrate, especially close to the IDTs. Thus, surfaces located between two neighboring electrode fingers are fully covered by these nanostructures. Aloof from the IDTs, the surface of the substrate is formed of regular nanograins (Fig. 6(b)).

These results suggest the existence of an additional device degradation mechanism, consisting in an alteration of the AlN layer. EDXS analyses confirm this assumption, showing that the O-content in the AlN film dramatically increased during the experiment while the amount of nitrogen dropped (Fig. 7). With low-energy incident electrons (5 keV), the post-experiment N-content is even found to be null. If the energy is augmented to 20 keV, allowing the

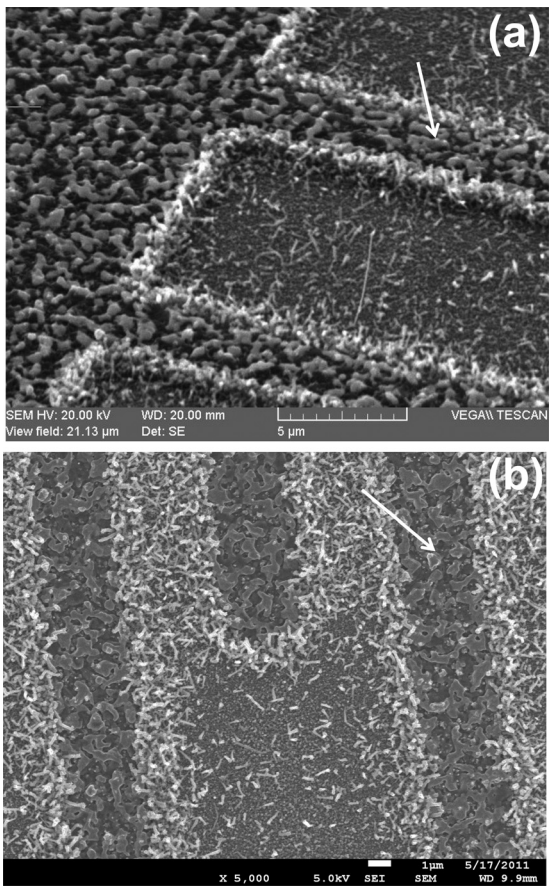

FIG. 6. Secondary electron SEM images of an Ir/AlN/Sapphire SAW device after the experiment: (a) tilted view, (b) plan view. The white arrows indicate the position of one finger electrode on each image for a better understanding.

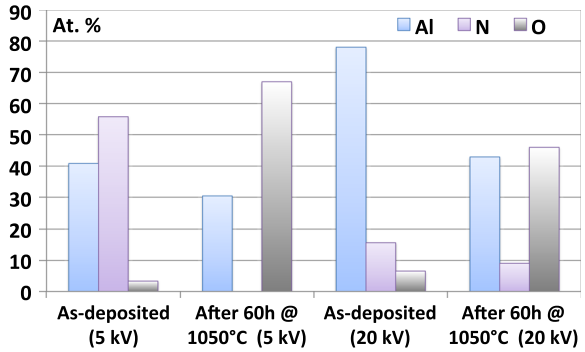

FIG. 7. Relative atomic compositions of the substrate before and after the experiment, determined by EDXS with 5 keV-electrons and 20 keV-electrons.

analysis of a deeper region, in exchange for a poorer accuracy in the determination of the quantities of light elements like O or N, then the N-content is close to 9%, to be compared with the initial measured level of about 15%. Note that these results are independent from the location of the examined areas—close or far away from the electrode fingers. Therefore, even under such low-O conditions (total pressure was 2.10^{-4} mbar), the AlN film surface underwent severe oxidation. Consequently, the nanostructures and nanograins visible on Fig. 6 are likely aluminum oxide of different microstructures.

A more accurate determination of the thickness and the microstructure of the oxide overlayer can be deducted from cross-sectional TEM images (Fig. 8). In zones located between neighboring electrode fingers, a 350 nm-thick oxide layer lying on the AlN film is clearly visible (Fig. 8(a)). It seems constituted of at least two parts (Fig. 8(b)). The upper part is identified as mainly amorphous Al_2O_3 (Fig. 8(c)). It corresponds to the nanostructures observed on SEM images (Fig. 6). The reason of the large concentration of these amorphous structures close to the electrode fingers is not clearly determined. The inner part, whose thickness is about 100 nm, is essentially textured α-Al_2O_3 (Fig. 8(d)). The electronic diffraction pattern of the highly textured AlN layer is also visible on this last figure. The nanograins visible in Fig. 6 aloof from the electrode fingers likely corresponds to this crystalized oxide layer.

D. Deterioration mechanisms during the plateau at 1050 °C

Based on these material analyses and the evolution of electrical parameters (IL and operating frequency) during the final plateau at 1050 °C (Fig. 5), a scenario leading to the device failure can be proposed. In particular, the IL evolution curve suggests that the device degradation takes place in two steps. Indeed, during the first 45 h at 1050 °C, IL evolution follows an exponential decay law, which means a progressive decrease of the degradation phenomena kinetics. Consequently, we assume that this first stage of the degradation is mainly related to the oxidation process underwent by the AlN layer. Actually, such kinetics is typical of oxidation processes, which are steadily hindered as the diffusion of O

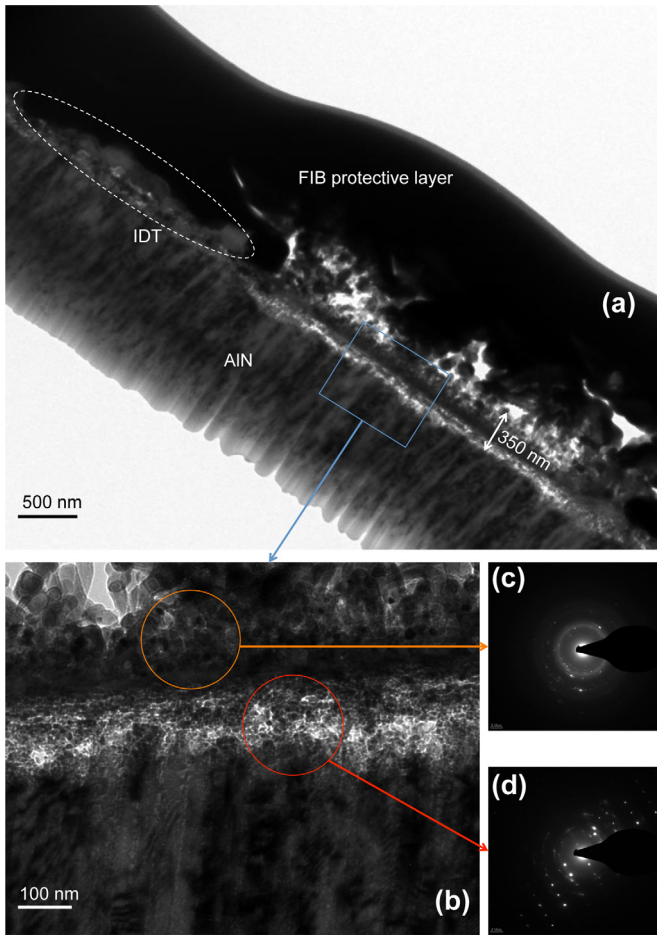

FIG. 8. (a) and (b) Cross-sectional TEM images of the device after the experiment. On top of the sample is visible the protective layer used to perform FIB cutting. (c) Electronic diffraction pattern of the upper part of the formed oxide overlayer. (d) Electronic diffraction pattern of the inner part of the formed oxide overlayer and the highly textured AlN layer.

atoms throughout the oxide overlayer becomes harder and harder with the increase of the oxide thickness.[21] The drift towards lower operating frequencies, which follows an exponential decay law as well, with a similar time constant close to 40 h, is a confirmation of the prevalence of the oxidation process during the first stage of the degradation (Fig. 5). Obtaining lower operating frequencies means that the formed oxide layer is softer than both AlN and sapphire, which is consistent with its partly amorphous nature. The second part of IL evolution, occurring after 45 h at 1050 °C, with a brutal acceleration of the degradation leading to the signal loss 15 h later (Fig. 5), would be then mainly driven by the agglomeration phenomena taking place in the Ir IDTs. Note that agglomeration phenomena should not have a major impact on the operating frequency, the mass loading effect being unchanged. Thus, the exponential decay of the operating frequency, related to the ongoing oxidation process, continues during this second stage, except at the very end of the experiment, after 55 h at 1050 °C (Fig. 5). At this time, the signal magnitude was close to the noise level, preventing an accurate determination of the operating frequency.

According to this scenario, the oxidation process is not responsible of the device failure but precludes the aimed

sensor applications, at least at such extreme temperatures. In that case, AlN-based devices could only be considered if the AlN layer was protected from oxygen. In this context, Al_2O_3/IDT/AlN/sapphire or Al_2O_3/AlN/IDT/AlN/sapphire configurations are promising solutions to protect concurrently IDTs from agglomeration phenomena and the active piezoelectric area from any chemical aggression.[22,23] Moreover, using such buried IDTs structures would significantly improve the electromechanical coupling coefficient.[24] For applications at lower temperatures, i.e., below 1000 °C, conventional IDT/AlN/Sapphire structures could be used for sensors applications, depending on the oxygen partial pressure and the aimed temperature range.

IV. CONCLUSION

In summary, AlN/sapphire SAW delay lines have been characterized at high temperatures under vacuum conditions. They showed a large and quasi-linear sensitivity to the temperature, as well as stable signals with variations below 3 dB during the 15-h-long heating from room temperature to 1050 °C. This combination makes AlN/sapphire bilayer structure a promising candidate for wireless SAW temperature sensing applications in harsh environments. However, despite the low-O conditions, a significant oxidation of the AlN film was evidenced by SEM, TEM, and EDXS. This phenomenon occurred during the 60-h-long plateau at 1050 °C and implied a regular increase of IL as well as operating frequency drift. AlN-based SAW devices can only be considered for the aimed applications if the targeted temperature range is lower than 1000 °C (depending on the O partial pressure) or if the active piezoelectric AlN layer is protected from oxygen, using buried electrodes configurations.

ACKNOWLEDGMENT

This work has been supported by the "Region Lorraine, CONTRAT DE PROJET ETAT-REGION 2007–2013; Pôle de Recherche Scientifique et Technologique. Matériaux, Energie, Procédés, Produits: Matériaux fonctionnels micro- et nanostructurés pour la réalisation de micro-et nano-systèmes."

[1]R. Fachberger, G. Bruckner, R. Hauser, and L. Reindl, in *Proceedings of IEEE International Frequency Control Symposium* (2006), p. 358.
[2]M. P. da Cunha, R. J. Lad, T. Moonlight, G. Bernhardt, and D. J. Frankel, Proc.-IEEE Ultrason. Symp. **2008**, 205.
[3]T. Aubert, J. Bardong, O. Elmazria, G. Bruckner, and B. Assouar, IEEE Trans. Ultrason. Ferroelectr. Freq. Control **59**, 194 (2012).
[4]R. Fachberger, G. Bruckner, R. Hauser, C. Ruppel, J. Biniasch, and L. Reindl, Proc.-IEEE Ultrason. Symp. **2**, 1223 (2008).
[5]M. P. da Cunha, R. J. Lad, T. Moonlight, S. Moulzolf, A. Canabal, R. Behanan, P. M. Davulis, D. Frankel, G. Bernhardt, T. Pollard, and D. F. McCann, Proc. IEEE Sens. **2011**, 614.
[6]J. Hornsteiner, E. Born, G. Fischerauer, and E. Riha, in *Proceedings of IEEE International Frequency Control Symposium* (1998), p. 615.
[7]D. Damjanovic, Curr. Opin. Solid State Mater. Sci. **3**, 469 (1998).
[8]N. D. Patel and P. S. Nicholson, NDT Int. **23**, 262 (1990).
[9]O. Ambacher, M. S. Brandt, R. Dimitrov, T. Metzger, M. Stutzmann, R. A. Fisher, A. Miehr, A. Bergmaier, and G. Dollinger, J. Vac. Sci. Technol. B **14**, 3532 (1996).
[10]T. Aubert, O. Elmazria, B. Assouar, E. Blampain, A. Hamdan, D. Genève, and S. Weber, IEEE Trans. Ultrason. Ferroelectr. Freq. Control **59**, 999 (2012).
[11]C. Caliendo, Appl. Phys. Lett. **83**, 4851 (2003).
[12]M. B. Assouar, O. Elmazria, P. Kirsch, P. Alnot, V. Mortet, and C. Tiusan, J. Appl. Phys. **101**, 114507 (2007).
[13]C. M. Lin, T. T. Yen, V. V. Felmetsger, M. A. Hopcroft, J. H. Kuypers, and A. P. Pisano, Appl. Phys. Lett. **97**, 083501 (2010).
[14]G. Bruckner, J. Bardong, R. Fachberger, E. Forsén, and D. Eisele, in *Proceedings of IEEE International Frequency Control Symposium* (2010), p. 499.
[15]T. Aubert, O. Elmazria, B. Assouar, L. Bouvot, M. Hehn, S. Weber, M. Oudich, and D. Geneve, IEEE Trans. Ultrason. Ferroelectr. Freq. Control **58**, 603 (2011).
[16]J. Bardong, G. Bruckner, G. Franz, R. Fachberger, and A. Erlacher, in *Proceedings of IEEE International Frequency Control Symposium* (2009), p. 28.
[17]M. Lisker, T. Hur'yeva, Y. Ritterhaus, and E. P. Burte, Surf. Coat. Technol. **201**, 9294 (2007).
[18]T. Aubert, M. B. Assouar, O. Legrani, O. Elmazria, C. Tiusan, and S. Robert, J. Vac. Sci. Technol. A **29**, 021010 (2011).
[19]R. Farrell, V. R. Pagán, A. Kabulski, S. Kuchibhatla, J. Harman, K. R. Kasarla, L. E. Rodak, J. Hensel, P. Famouri, and D. Korakakis, *High Temperature Annealing Studies on the Piezoelectric Properties of Thin Aluminum Nitride Films* (Mater. Res. Soc. Symp. Proc., 2007), Paper No. 1052-DD06-18.
[20]R. M. Tiggelaar, R. G. P. Sanders, A. W. Groenland, and J. G. E. Gardeniers, Sens. Actuators, A **152**, 39 (2009).
[21]H. C. Kang, S. H. Seo, J. W. Kim, and D. Y. Noh, Appl. Phys. Lett. **80**, 1364 (2002).
[22]O. Legrani, O. Elmazria, A. Bartasyte, T. Aubert, and A. Talbi, Proc.-IEEE Ultrason. Symp. 2102 (2012).
[23]T. Aubert, O. Elmazria, B. Assouar, L. Bouvot, and M. Oudich, Appl. Phys. Lett. **96**, 203503 (2010).
[24]C. Caliendo, Appl. Phys. Lett. **92**, 033505 (2008).